AGU PUBLICATIONS

JGR

Journal of Geophysical Research: Earth Surface

RESEARCH ARTICLE
10.1002/2015JF003780

Key Points:
- Model of waves and river mouth morphodynamics shows littoral bypassing and river mouth migration
- Bypassing pathways through river mouth bar migration, spit breaching, and channel dynamics
- Effects on spit width and bypassing make migration fastest for intermediate river discharge

Supporting Information:
- Supporting Information S1
- Animation S1
- Animation S2
- Animation S3
- Animation S4
- Animation S5

Correspondence to:
J. H. Nienhuis,
jnienhui@tulane.edu

Citation:
Nienhuis, J. H., A. D. Ashton, W. Nardin, S. Fagherazzi, and L. Giosan (2016), Alongshore sediment bypassing as a control on river mouth morphodynamics, *J. Geophys. Res. Earth Surf.*, *121*, 664–683, doi:10.1002/2015JF003780.

Received 4 NOV 2015
Accepted 31 MAR 2016
Accepted article online 6 APR 2016
Published online 21 APR 2016

Alongshore sediment bypassing as a control on river mouth morphodynamics

Jaap H. Nienhuis[1,2], Andrew D. Ashton[1], William Nardin[3], Sergio Fagherazzi[3], and Liviu Giosan[1]

[1]Department of Geology and Geophysics, Woods Hole Oceanographic Institution, Woods Hole, Massachusetts, USA, [2]Earth, Atmospheric and Planetary Sciences, Massachusetts Institute of Technology, Cambridge, Massachusetts, USA, [3]Department of Earth and Environment, Boston University, Boston, Massachusetts, USA

Abstract River mouths, shoreline locations where fluvial and coastal sediments are partitioned via erosion, trapping, and redistribution, are responsible for the ultimate sedimentary architecture of deltas and, because of their dynamic nature, also pose great management and engineering challenges. To investigate the interaction between fluvial and littoral processes at wave-dominated river mouths, we modeled their morphologic evolution using the coupled hydrodynamic and morphodynamic model Delft3D-SWAN. Model experiments replicate alongshore migration of river mouths, river mouth spit development, and eventual spit breaching, suggesting that these are emergent phenomena that can develop even under constant fluvial and wave conditions. Furthermore, we find that sediment bypassing of a river mouth develops though feedbacks between waves and river mouth morphology, resulting in either continuous bypassing pathways or episodic bar bypassing pathways. Model results demonstrate that waves refracting into the river mouth bar create a zone of low alongshore sediment transport updrift of the river mouth, which reduces sediment bypassing. Sediment bypassing, in turn, controls the river mouth migration rate and the size of the river mouth spit. As a result, an intermediate amount of river discharge maximizes river mouth migration. The fraction of alongshore sediment bypassing can be predicted from the balance between the jet and the wave momentum flux. Quantitative comparisons show a match between our modeled predictions of river mouth bypassing and migration rates observed in natural settings.

1. Introduction

River mouths carry out a pivotal role in Earth-surface dynamics by transporting most of the sediment eroded from the continents to the oceans [*Hay*, 1998]. Sediment delivered to the coast steadily shapes our densely populated coastlines and deltas [*Boyd et al.*, 1992]. As such, river mouths are the nexus of delta formation, representing the location of first response to fluvial sediment fluctuations, as the river mouth morphology rapidly adapts to anthropogenic sediment reduction and climate change [*Syvitski and Saito*, 2007; *Nienhuis et al.*, 2013]. A well-known example is the Nile River mouth at Rosetta that has been retreating at an average rate of 58×10^4 m yr^{-1} as a result of the Aswan Dam construction in 1964 [*Stanley and Warne*, 1998]. The importance of ocean wave action on river mouth morphology has long been recognized [*Wright*, 1977]; however, the effect of waves on river mouth morphodynamics is in a stage of nascent understanding [*Giosan*, 2007; *Nardin and Fagherazzi*, 2012; *Nardin et al.*, 2013; *Fagherazzi et al.*, 2015]. Quantifying the drivers of river mouth morphology in the presence of waves is not only important for forecasting upcoming changes to our deltaic shorelines but also allows us to better understand the long-term coupling of terrestrial and marine processes.

Here we study how waves and associated alongshore sediment transport affect river mouth morphology and how river mouth dynamics can be quantified in a framework of alongshore sediment bypassing, alongshore river mouth migration, and river mouth spit breaching. We test this framework with model experiments of self-formed river mouth morphology in idealized environments on yearly to decadal timescales using the numerical model Delft3D-SWAN [*Deltares*, 2014]. We then apply the alongshore sediment bypassing and river mouth migration parameterizations we have derived from Delft3D experiments to a selection of natural examples.

2. Background

2.1. River Mouths in the Absence of Waves

When a river enters a standing body of water, its discharge and sediment load, previously confined to the channel, form a river mouth jet that gradually slows down and expands [*Bates*, 1953; *Wright*, 1977; *Canestrelli*

et al., 2014; *Fagherazzi et al.*, 2015]. Hydrodynamically, river mouth jets are turbulent and bounded above and below by the free surface and bed friction, respectively [*Rowland et al.*, 2009; *Canestrelli et al.*, 2014]. Dynamics of river mouths and their sedimentary deposits depend on the relative densities of the river and basin waters, the inertia of the river flow, and bed friction [*Bates*, 1953]. Depending on these environmental factors, river mouth jets can be unstable and meandering [*Jirka*, 1994; *Mariotti et al.*, 2013; *Canestrelli et al.*, 2014], can plunge below the basin water (hyperpycnal flow conditions), or be buoyant (hypopycnal flow conditions) [*Bates*, 1953; *Wright*, 1977].

The hydrodynamics of river mouths are strongly coupled to their morphology and morphodynamics. River mouth width and depth are a function of fluvial discharge, sediment characteristics, and bank cohesion [*Wright*, 1977; *Parker*, 1978; *Andren*, 1994]. Sediment from the decelerating river mouth jet can be preferentially deposited as a mouth bar in the jet centerline or as levees along the sides of the jet, depending on jet stability and bed friction [*Rowland et al.*, 2010; *Mariotti et al.*, 2013; *Canestrelli et al.*, 2014; *Falcini et al.*, 2014].

2.2. Wave Effect of River Mouths

Most often, river mouths are shaped not only by fluvial factors but also by marine processes such as waves and tides. Waves affect the river mouth jet by increasing bed friction, which enhances jet spreading [*Ismail and Wiegel*, 1983] and jet stability [*Jirka*, 2001]. *Ismail and Wiegel* [1983], using theory and laboratory experiments, demonstrated that jet spreading is controlled by the ratio between wave momentum and jet momentum. Waves make river mouth bars form closer to the river mouth and impede the growth of lateral levees [*Wright*, 1977; *Nardin et al.*, 2013]. River mouth bars often form during floods, but channel bifurcations around river mouth bars are short-lived when waves are present [*Giosan et al.*, 2005; *Gelfenbaum et al.*, 2015], resulting in the formation of one major channel [*Jerolmack and Swenson*, 2007]. Wave-dominated river mouths not only display depositional patterns very similar to ebb-tidal deltas offshore of tidal inlets [*Fitzgerald*, 1982] but also generate unique features such as large submarine platforms [*Giosan et al.*, 2005; *Giosan*, 2007]. The most obvious effect of waves on river mouths is expressed in the large-scale plan-view morphology of wave- versus river-dominated deltas; wave-driven alongshore sediment transport spreads sediment from the river mouth alongcoast to produce cuspate deltas with smooth shorelines [*Nienhuis et al.*, 2015b].

When waves approach the river mouth obliquely, they set up an alongshore current. This alongshore current and the associated transport of sediment interacts with the jet, such that shoals and subaqueous levees mostly form on the updrift side [*Wright*, 1977; *Giosan*, 2007] and extensive deltaic submarine platforms mostly form on the downdrift side [*Correggiari et al.*, 2005; *Giosan et al.*, 2005]. Waves can also deflect the river mouth jet even in the absence of an established alongshore current [*Nardin and Fagherazzi*, 2012]. *Tanaka et al.* [1996] show that the balance between river mouth sediment deposition by littoral processes and sediment erosion by fluvial discharge controls the width and depth of river mouths in wave-dominated environments. In some cases, when the discharge of individual streams is too small to maintain a permanent river mouth, rivers can amalgamate alongshore until the outlet has sufficient discharge to maintain a permanent river mouth [*Zenkovich*, 1967].

The morphology and sediment composition of river mouths on coasts with a net direction of littoral (or alongshore) transport are often asymmetrical (i.e., different on the updrift and downdrift coasts) because two sediment sources feed delta mouths: fluvial and littoral [*Giosan*, 1998]. Waves are an efficient sediment sorter and move fine-grained fluvial material offshore, coarsening the nearshore environment [*Friedman*, 1967]. The dynamics of wave-dominated river mouths thus depend on how the fluvial sediment interfaces with sediment sourced from the updrift coastline [*Hicks and Inman*, 1987].

2.3. Sediment Bypassing and River Mouth Migration

Important in the interaction between alongshore sediment transport and river discharge is how sediment is potentially able to bypass the river mouth [*Zenkovich*, 1967]. Using sediment tracers, *Aibulatov and Shadrin* [1961] found that littoral sediment was transported around the river mouth bar. In another study, *Balouin et al.* [2006] identified a littoral sediment bypass pathway through the river mouth channel. Littoral bypassing around river mouths bears many similarities with bypassing around tidal inlets. *Bruun and Gerritsen* [1959] found that for high ratios of littoral transport to tidal discharge, strong waves force bypassing around the ebb tidal delta. For a low littoral transport relative to tidal discharge, waves are weak, and tidal currents transport littoral sediment via the channel and the ebb-tidal delta to the downdrift coast. *Dodet et al.* [2013] attributed the relationship between tidal discharge and the alongshore current to wave-current

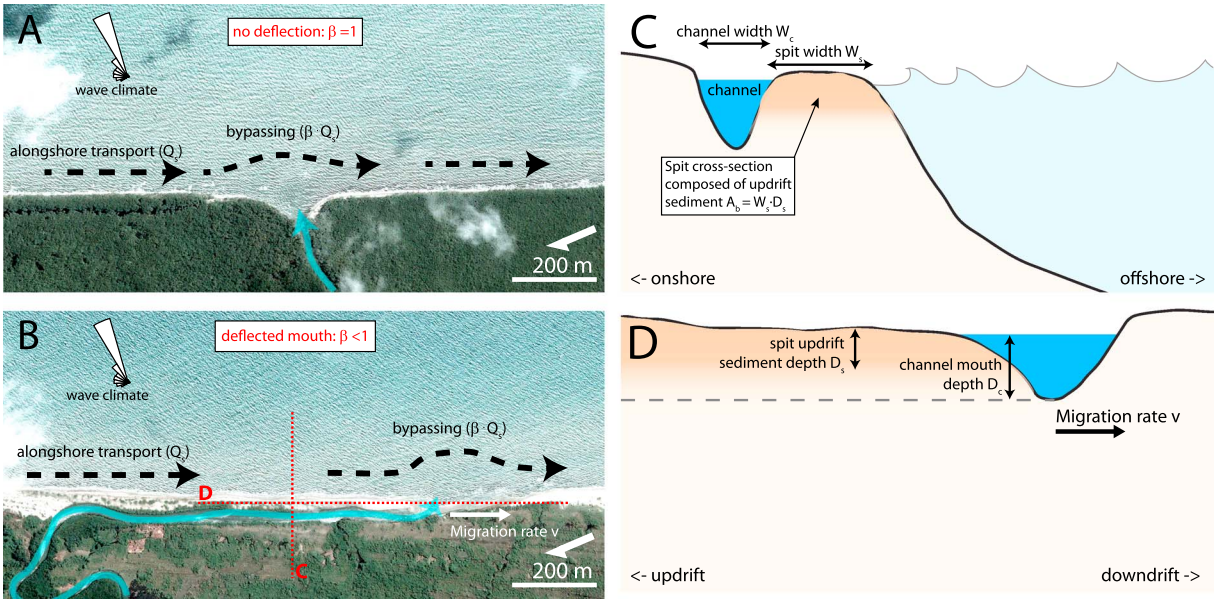

Figure 1. Examples of two wave-dominated river mouths. (a) An undeflected mouth of the Sikia Pakia Bila River and (b) a deflected mouth of the Dakura Tingni River, both along the coast of Nicaragua and experiencing a similar wave climate. The red dotted lines indicate the orientations of the schematized cross sections of Figures 1c and 1d. The wave roses display the angular distribution of wave energy using data from WaveWatch III® [*Chawla et al.*, 2013]. Images © Google Earth. (c) A schematized cross section of the river mouth spit of Figure 1b, illustrating the sediment supplied by alongshore transport from the updrift coast as the updrift sediment cross-sectional area A_b. (d) A schematized along section of the river mouth spit of Figure 1b, highlighting the difference between the channel depth at the river mouth and the spit updrift sediment depth.

interactions such as wave blocking and alongshore current disorganization. *Rodriguez et al.* [2000] suggested that suspended sediment could further dissipate waves around river mouths and limit alongshore sediment transport. See also *Anthony* [2015] for a recent review on the wave influence of river deltas.

Reductions in alongshore sediment bypassing affect the long-term morphology of a river mouth (Figure 1) [see also *Zenkovich*, 1967; *Dominguez*, 1996]. If the river mouth acts as an obstacle to the alongshore transport and no sediment is able to bypass, a river mouth spit tends to form that can cause the channel to migrate downdrift (Figure 1b). For example, the river mouth spit on the Senegal river is 26 km long and migrated an average of 200×10^4 m yr^{-1} between 1850 and 1917 [*Guilchar and Nicholas*, 1954]. While river mouth processes and alongshore sediment bypassing control the initial formation of river mouth spits, subsequent subaerial accretion of the spit is caused by onshore sand transport, wind, and vegetation [*Sedrati et al.*, 2011; *Heathfield and Walker*, 2015].

There are limits, however, to the distance that river mouths can migrate alongshore. In cases where the river mouth spit is coarse grained such that groundwater flow is significant, discharge through the mouth decreases as the barrier elongates. A reduced river mouth discharge can then lead to either mouth closure or significant bypassing of sediment around the mouth, which would stop migration [*Kirk*, 1991; *Balouin et al.*, 2006]. Another natural limit to migration is spit breaching caused by storms or floods. Breaching events "reset" the river mouth updrift; this rapid change of the river outlet can be seen as a large instantaneous bypassing event [*Cooper*, 1990; *Kirk*, 1991; *Hart*, 2007]. A spit breach leaves behind a lagoon: a depression where once the channel flowed through [*Hart*, 2007]. *Kelk* [1974] demonstrated that the Ashburton River in New Zealand exhibits cycles of alongshore migration and subsequent spit breaching of about 12–19 months.

When river mouths carry significantly larger fluvial sediment supply, they can reorient the coastline into a cuspate wave-dominated delta [*Nienhuis et al.*, 2015b] and make the dynamics of alongshore sediment bypassing and river mouth migration more complicated [*Giosan*, 2007; *Anthony*, 2015]. In this case, different shoreline orientations on either side of the river mouth result in different quantities of alongshore sediment transport to and from the river mouth [*Bakker and Edelman*, 1964; *Ashton and Giosan*, 2011]. Interactions among fluvial sediment supply, the shoreline, and the directional wave climate develop such that alongshore sediment bypassing affects the channel orientation and can control updrift versus downdrift flank growth [*Nienhuis*, 2016]. One example is the undeflected St. George lobe of the Danube delta. Here *Giosan et al.*

[2005] show that an efficient bypassing mechanism exists where littoral sediment is initially trapped in front of the river mouth but in time is transported downdrift when a barrier island emerges.

2.4. Models of River Mouth Morphodynamics

Several numerical models of river mouth dynamics have been developed, in some cases to estimate future river mouth geometries [*Tanaka*, 2003] or in others to explain the physics behind observed river mouth morphologies [*Edmonds and Slingerland*, 2007; *Gelfenbaum et al.*, 2015]. *Gelfenbaum et al.* [2015] modeled the hydrodynamics and sediment transport of the Elwha River delta to match real-time measurements. In their study, they simulated 2 months of morphologic change of the delta following the removal of a dam in the river watershed. Simpler, predictive models of river mouths can incorporate only a few processes, such as *Tanaka*'s [2003] model of the competition between alongshore sediment transport closing the river mouth and fluvial currents eroding the river mouth. Such a simple model allows for the implementation of more realistic boundary conditions on longer timescales.

Here we choose an intermediate approach, similar to that of *Edmonds and Slingerland* [2007] and *Nardin et al.* [2013], where we use a detailed simulation model (Delft3D-SWAN) [see *Deltares*, 2014] to simulate idealized river mouth morphodynamics over interannual timescales. We model the morphologic development of river mouths under the influence of waves, where the river interacts with a sandy shoreline and a fully developed littoral current. A critical aspect of our simulations is that the river mouth morphology is an emergent characteristic of the underlying physics. Although model complexity limits us to the use of only simple boundary conditions, it does allow a detailed exploration of the physics of river mouths. We then draw on our model experiments to parameterize a simple conceptual model of sediment bypassing and river mouth spit evolution that we subsequently test against natural examples.

3. Conceptual Model of Sediment Bypassing

To analyze our model experiments and to explore the effect of wave and fluvial dynamics on alongshore sediment bypassing and channel migration, we propose a conceptual model of river mouths in wave-dominated environments (Figure 1). In this conceptual model, we quantify sediment bypassing as the fraction β of the net alongshore sediment transport (Q_s) that is transported across the river mouth [*Nienhuis et al.*, 2015a].

If there is a net direction of alongshore sediment transport and the river mouth is not migrating (Figure 1a), 100% of the littoral sediment must be able to bypass the river mouth ($\beta = 1$). If, on the other hand, a river mouth is migrating (Figure 1b), β must necessarily be less than 1 because some sediment must build the spit causing mouth migration. River mouth migration and river mouth spit formation are therefore closely coupled; river mouths migrate by building a river mouth spit, and the river mouth spit forms because the river mouth itself migrates alongshore.

When fluvial sediment supply is small relative to the alongshore sediment transport, the river is not able to reorient the shoreline (Figure 1) [*Nienhuis et al.*, 2015b]. In this case, we can infer the alongshore sediment bypassing fraction β from the migration rate of the river mouth, invoking the conservation of mass:

$$v = \frac{Q_s \cdot (1 - \beta)}{A_b}, \tag{1}$$

where v is the migration rate (ms^{-1}), Q_s is the volumetric alongshore sediment transport rate ($m^3\,s^{-1}$), β is the fraction of alongshore sediment transport that is able to bypass the river mouth, $A_b = W_s \cdot D_s$ is the cross-sectional area of the river mouth spit (m^2) composed of blocked littoral sediment from the updrift coast, W_s is the width of the spit, and D_s is spit updrift sediment depth (Figures 1c and 1d). Because bypassing is defined relative to the alongshore location of the river mouth, a breaching event would entail a large sudden increase in the volume of sediment bypassed.

For deltaic systems where relative fluvial sediment supply is larger, a break in the shoreline orientation develops across the river mouth [*Grijm*, 1960; *Bakker and Edelman*, 1964; *Ashton and Giosan*, 2011]. In this case, bypassing is expected to play an important role in controlling the channel orientation due to feedbacks between fluvial sediment supply, the bypassing fraction β, and the offshore wave climate. For example, *Nienhuis* [2016] prescribed an alongshore sediment bypassing fraction in a simplified model of shoreline evolution and found that bypassing plays an important role in large-scale delta dynamics; however, as arbitrary values of β were

used, they did not explore the processes controlling alongshore sediment bypassing. Here we formulate and test a quantitative framework of river mouth bypassing that can be applied to large-scale deltas in wave-dominated environments.

4. Methods

4.1. Delft3D-SWAN

To explore the morphodynamics of wave-dominated river mouths, we use the coupled hydrodynamic and morphodynamic model Delft3D-SWAN [*Lesser et al.*, 2004]. Delft3D solves the shallow water equations for unsteady, incompressible, and turbulent flow. We use Delft3D in two dimensions, solving the depth-averaged flow. The Delft3D flow model is embedded in the SWAN phase-averaged spectral wave model which solves the wave action equation to simulate wave propagation and dissipation as well as wave-wave and wave-current interactions [*Booij et al.*, 1999]. We use the formulations of *van Rijn* [1993] to calculate suspended and bed load sediment transport due to the waves and currents. In this depth-averaged model, we set the wave-related suspended and bed load transport factors to 0.15 in order to reduce unrealistic shoreface steepening [*Brocatus*, 2008].

4.2. Model Setup

We explore river mouth morphodynamics with an idealized initial shoreface and river mouth (Figure 2). The Delft3D flow domain is 6 km alongshore and 5 km offshore and includes a 750 m wide subaerial beach elevated 3 m above mean sea level to prevent overland flow. The grid resolution is 40 m in the alongshore direction and 25 m, 50 m, and 100 m in the cross-shore direction depending on water depth. We set a high grid resolution to ensure that the alongshore current is at least seven grid cells wide. Tests with an even finer grid show that there is a negligible effect of the resolution on the modeled river mouth morphology (Figure S3 in the supporting information). The entire flow domain is 150×116 cells, with an offshore water level boundary condition and two alongshore Neumann boundary conditions that allow the alongshore current and associated sediment transport to freely flow into and out of the domain [*Deltares*, 2014]. The channel is forced with a discharge boundary condition, with water that has equal density as the basin water. Fluvial sediment is supplied as a constant sediment concentration condition at the same boundary. The flow domain is embedded in a slightly larger "small" SWAN wave domain that extends alongshore for 30 km within a "large" SWAN wave domain that encompasses 186 km alongshore by 90 km offshore (Figure 2b). A wave domain of this size allows for a fully developed alongshore current without boundary artifacts [*List and Ashton*, 2007].

The initial shoreface follows a Dean-type profile of $h(x) = a\,x^{2/3}$, where h is the water depth (m) at a distance x (m) from shore and a is 0.1, the recommended value for 200 μm sand [*Dean*, 1991]. We extend this shape offshore to 200 m depth in the wave domain (Figure 2c), an extension well beyond the shallow closure depths ($<$10 m) used to develop this shape; however, the deeper profile is nearly linear and does not affect model behavior, particularly as waves at the offshore boundary are well within deep water. The initial river mouth is straight and shore perpendicular, shallowing toward the beach to limit the river mouth's offshore expression (Figure 2a). We use simple hydraulic geometry relations [*Parker*, 1978] to initialize the river channel dimensions for the given discharge condition at the boundary to limit spin-up effects. The river banks are fully erodible.

The initial bed composition of the model domain consists of 200.01 μm "updrift sediment," located updrift of the initial river mouth and 200.00 μm "downdrift sediment," located downdrift of the initial river mouth (Figure 2a). Supplied fluvial sediment consists of 199.99 μm sand. With this minimal but detectable grain size variation and by tracking the bed composition using 25 vertical cells of 0.2 m each, sediment acts as a tracer. This allows us to track the movement of the updrift, downdrift, and fluvial sediment "fractions" as the delta mouth morphology evolves while making sure that each fraction has nearly equal transport properties.

All model experiments have long-period deep water swell waves approaching 40° from shore normal (Figure 2), with a wave period of 10 s and with wave heights varied between 0.7 m and 1.5 m, setting up alongshore sediment transport rates (Q_s) between 7 and 70 kg s^{-1}. Water discharge is varied between 50 m^3 s^{-1} and 2000 m^3 s^{-1}; fluvial sediment supply is varied between 0 kg s^{-1} and 50 kg s^{-1}. Even though almost all natural river mouths carry some fluvial sediment, we include model experiments without fluvial sediment supply to simplify the long-term mass balance of the littoral system. Note that the absence of fluvial sediment supply

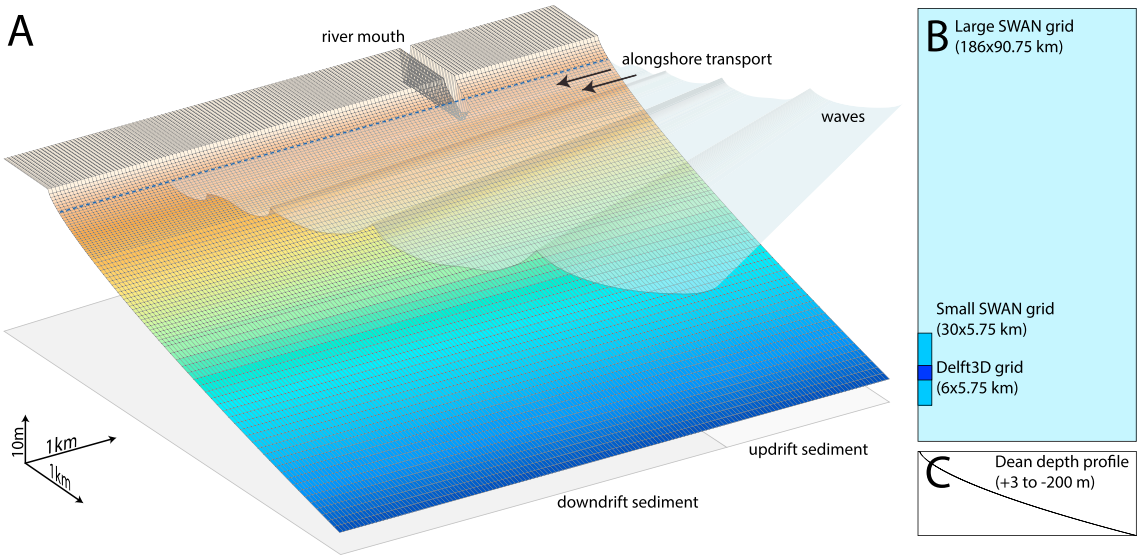

Figure 2. (a) The Delft3D flow domain and (b) the flow domain embedded into a two larger SWAN wave domains. The initial subaerial beach is 750 m wide and 3 m above mean sea level. (c) Initial cross-shore profile.

can introduce scour at the upstream boundary. See supporting information Table S1 for overview of all the settings and parameters. Supporting information Table S2 lists all the model experiments.

We run the model with 1 day of hydrodynamic spin-up time and then do a fully coupled hydrodynamic and morphodynamic simulation of 13 days. We use a morphologic scaling factor to speed up the morphodynamics [*Lesser et al.*, 2004], multiplying bed erosion and deposition with a linear factor of 90; tests with morphologic factors of 22.5 and 45 show that a factor of 90 does not significantly affect the morphodynamics. Because of the morphologic factor, our 13 day hydrodynamic simulations correspond to approximately 3.2 years of morphologic change.

4.3. Model Analyses

We use the model setup as described above to investigate wave effects on river mouth morphology, bypassing, and migration. The river mouth dimensions, the river mouth jet, and the alongshore sediment transport are emergent properties of the simulation that codevelop with the morphology. To compute bypassing, we track the position of the channel through time, from the upstream boundary (river apex) to the location of minimum depth along the channel (river mouth). The cumulative alongshore sediment bypassing fraction β is,

$$\beta_{\text{cumulative}} = \frac{V_{\text{u,d}}}{V_{\text{u}}}, \tag{2}$$

where $V_{\text{u,d}}$ is the volume (m^3) of the updrift sediment fraction that is located downdrift of the river mouth, including the updrift sediment that has left the domain. V_{u} is the cumulative volume (m^3) of updrift sediment that has been brought into the domain across the updrift boundary.

The instantaneous bypassing fraction β_{inst} is,

$$\beta_{\text{instantaneous}} = \frac{Q_{\text{u,d}}}{Q_{\text{u}}} = \frac{\Delta V_{\text{u,d}}/\Delta t}{\Delta V_{\text{u}}/\Delta t}, \tag{3}$$

where $Q_{\text{u,d}}$ is the updrift fraction sediment flux ($m^3\,s^{-1}$) that is bypassing the river mouth. Q_{u} is the updrift fraction sediment flux ($m^3\,s^{-1}$) updrift of the river mouth, which is equal to the sediment flux brought into the domain along the upstream boundary. To calculate $\beta_{\text{instantaneous}}$, we measure the change in time of $V_{\text{u,d}}$ and V_{u}. Because we calculate $V_{\text{u,d}}$ and V_{u} at each hydrodynamic time step of 0.2 min and the model has a morphologic scaling factor of 90, the time interval Δt over which we calculate $\beta_{\text{instantaneous}}$ is 18 min.

Note that while the cumulative bypassing fraction β for downdrift migrating river mouths is always between 0 and 1, the instantaneous fraction can be much greater than 1, for example, when a spit breaches and the river mouth

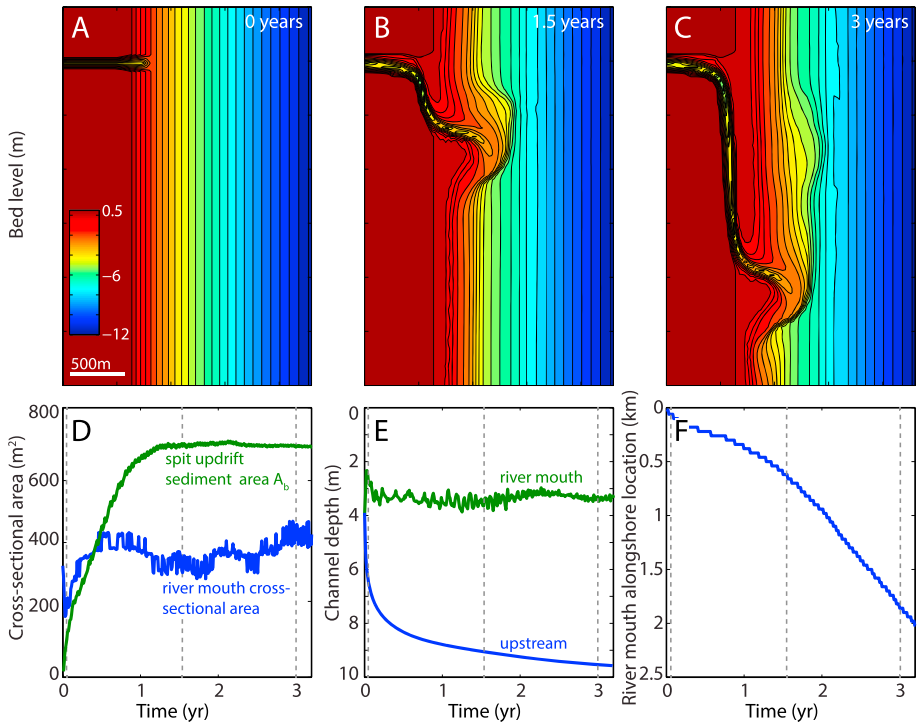

Figure 3. Close-up view of a typical model experiment after (a) 0, (b) 1.5, and (c) 3 years. Time evolution of basic river mouth properties, (d) the cross-sectional area of the spit updrift sediment and the river mouth, (e) the channel depth and the upstream boundary and at the river mouth, and (f) the river mouth alongshore location. Dashed lines indicate moments of snapshots shown in Figures 3a–3c. Fluvial discharge $Q = 200\ m^3\ s^{-1}$, fluvial sediment supply $Q_r = 0\ kg\ s^{-1}$, and offshore wave height $H_s = 1$ m.

relocates upcoast. The instantaneous fraction can also be negative when the river mouth migrates into updrift sediment that bypassed previously. In this sense, we define "updrift" and "downdrift" sediment fractions based on how sediments are initially located updrift and downdrift of the river mouth (section 4.2). The alternative approach, to relabel the sediment as updrift or downdrift at each time step, is troublesome within Delft3D and requires a new bed composition file, and therefore a new "run," at each time step. Therefore, in terms of bypassing, we only track the updrift sediment fraction of the river mouth spit as it is bypassed, and we do not take into account the reverse bypassing behavior of the eroded downdrift river bank. We correct our migration rate for this reverse bypassing by only tracking the updrift sediment as it is incorporated into the river mouth spit (Figures 1c and 1d).

5. River Mouth Morphology

We performed model experiments to explore river mouth morphodynamics and alongshore sediment bypassing. In each simulation, the river mouth quickly reaches a steady state width and depth (Figures 3d and 3e). The scour upstream of the river mouth caused by the $0\ kg\ s^{-1}$ fluvial boundary condition (Figure 3e) creates a temporary fluvial sediment flux of $0.09\ kg\ s^{-1}$ towards the river mouth, negligible compared to the $18\ kg\ s^{-1}$ of alongshore sediment transport. The shoreface profile is stable (or quasi-stable) such that, updrift of the river mouth, cross-shore sediment transport is negligible and alongshore sediment transport at the domain boundaries remains nearly constant throughout the simulation (Figure 3). No sandbars develop outside of the zone influenced by the river mouth. We attribute this to the constant wave conditions and the depth-averaged approximation of shoreface processes in Delft3D [see *Deltares*, 2014]. Both the equilibrium channel morphology and shoreface stability are essential in our study of river mouth morphodynamics, allowing us to investigate model behavior arising from emergent, developed morphodynamic feedbacks rather than transient changes developed from an initially out-of-equilibrium configuration. During the morphologic model spin-up, alongshore sediment bypassing is high and then gradually reaches a steady regime (Figure 4). Because of this model spin-up, the cumulative bypassing fraction decreases over the course of most simulations.

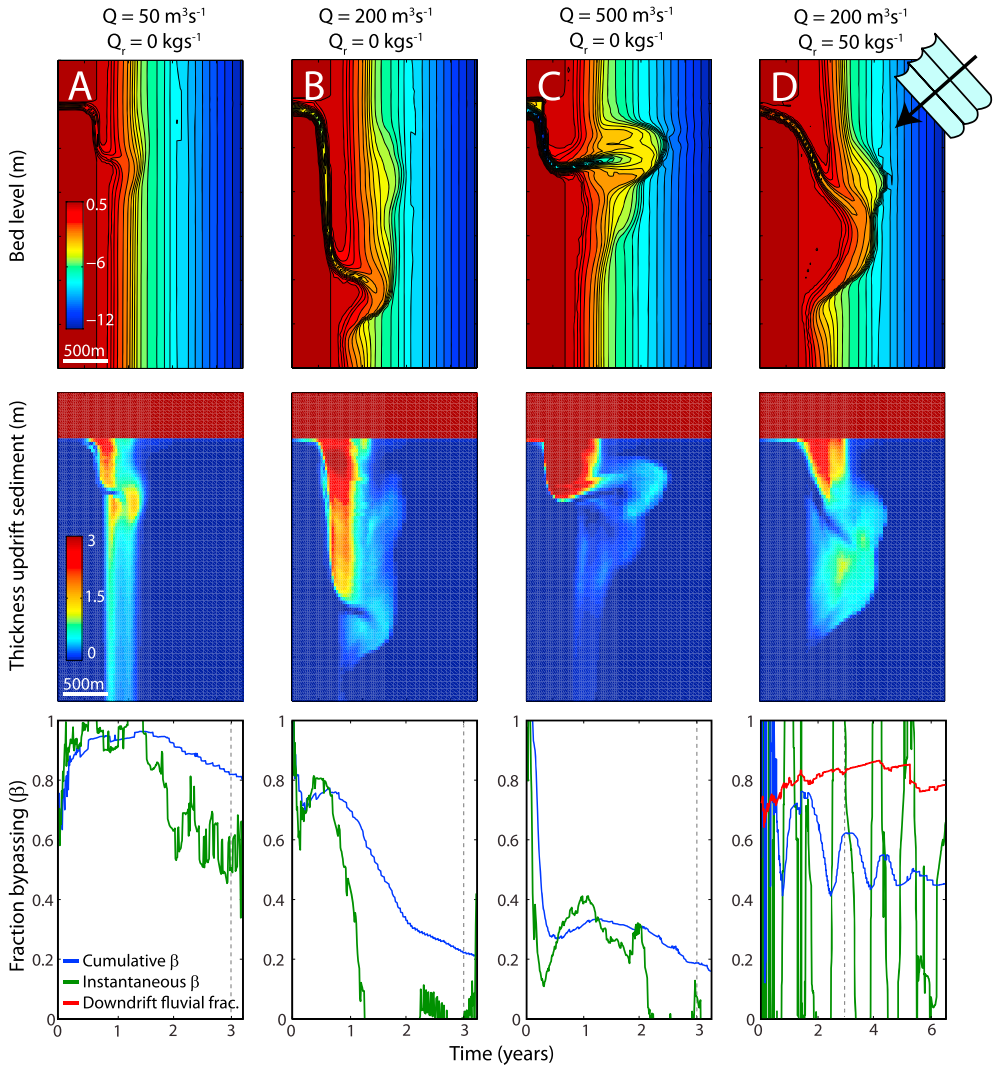

Figure 4. Close-up examples of (Figure 4, top) river mouth morphology and (middle) updrift sediment deposits after 3 years of sediment transport. See supporting information Animations S1–S4 for the full morphologic simulation. (bottom) The cumulative (blue) and the instantaneous (green) bypassing fraction along with the downdrift fraction of the fluvial sediment flux (red) through time. Wave height is 1 m, wave period is 10 s, and waves approach at −40° from normal.

Our results display a variety of river mouth morphologies depending on discharge and sediment supply (Figure 4). Broadly categorized, these morphologies include limited deflection (Figure 4a, see also Animation S1), deflected (Figure 4b, see also Animation S2), deflected with a river mouth oriented into the waves (Figure 4c, see also Animation S3), and a prograding asymmetric delta (Figure 4, see also Animation S4). For all simulations, by tracking the movement of updrift sediment, we can compute updrift sediment thickness and investigate its distribution across the domain (Figures 4a–4d, middle).

For the slightly deflected case (Figure 4a), the river mouth spit is small and consists mostly of updrift sediment. As such, littoral sediment is transported very effectively along the shore by breaking waves, easily bypassing the river mouth. For increasing discharge (Figures 4b and 4c), the river mouth bar increases in volume. The cumulative bypassing fraction is initially close to 1 but lowers throughout the duration of the simulation, dropping rapidly for simulations with a high discharge. A river mouth spit develops that causes the river mouth to migrate alongshore. The spit is elevated approximately 0.2 m above sea level in most simulations due to a combination of wave setup and a model threshold for drying of a grid cell. Interestingly, the rate of river mouth migration is maximized for the intermediate discharge scenario, while the alongshore sediment bypassing fraction continuously decreases for increasing discharge (Figure 5). This maximum in the river mouth migration rate occurs

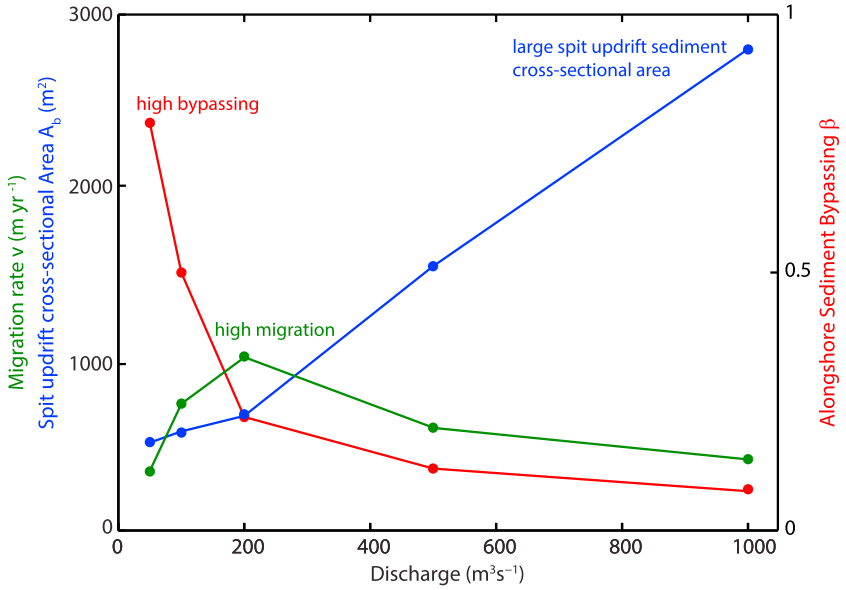

Figure 5. Average migration rate (green line), spit updrift sediment cross-sectional area (A_b) (blue line), and alongshore sediment bypassing fraction (red line) for model runs with different discharges and no sediment supply, $H_s = 1$ m, $T_p = 10$ s.

because the width of the river mouth spit increases for increasing discharge, lowering the migration rate even when bypassing is limited (equation (1) and Figure 5).

With a fluvial sediment supply, the shoreline protrudes seaward, developing a deltaic deposit with differing shoreline orientation between the updrift and downdrift flank (Figure 3d) [*Bhattacharya and Giosan*, 2003; *Ashton and Giosan*, 2011] and a downdrift-deflected channel [*Nienhuis*, 2016]. Bypassing is on average high ($\beta \sim 0.5$) but intermittent because of an unstable channel that oscillates periodically from a downdrift to an updrift orientation (Figure 4d, bottom, see also Animation S4). Apart from these oscillations, the river mouth migration rate is low compared to a river mouth without fluvial sediment supply. We attribute this difference in migration rate to the deposition of fluvial sediment downdrift of the river mouth. The growth of the downdrift beach leads to the initial low in alongshore sediment bypassing (compare the blue line in Figures 4b–4d) and the subsequent formation of an updrift delta flank composed of updrift sediment. Eventually, as the downdrift flank prevents further downdrift migration of the channel, bypassing increases to be higher than the model experiment without fluvial sediment supply (Figure 4b).

In general, the river mouth morphologies formed in the model arise from the interaction between fluvial discharge, the local wave field, and the alongshore sediment flux (Figure 6). Wave-current interactions and the presence of a river mouth bar steepen waves close to the river mouth and decrease the wave height updrift and downdrift of the river mouth (Figure 6).

6. Alongshore Sediment Bypassing

6.1. Bypassing Pathways

By tracing the instantaneous pathways of updrift sediment, model experiments show three mechanisms of alongshore river mouth sediment bypassing (Figure 6). One pathway, associated with low fluvial discharge and a weak river mouth jet that is highly deflected, arises when the channel depth is smaller than the breaking wave depth. In this case, the jet is easily deflected, and it has little impact on the incoming waves that drive alongshore sediment transport. Most of the updrift sediment is bypassed around a small river mouth bar, and there is minimal river mouth migration (Figures 4a and 6a).

In the second scenario, with a stronger river mouth jet and a larger river mouth bar (Figures 4b and 6b), alongshore sediment transport decreases close to the river mouth. A fraction (β) of the updrift sediment is conveyed into the channel and continues its way downdrift. The blocked (1-β) fraction of the updrift supply, however, deposits at the river mouth spit, forcing the river mouth to migrate downdrift. Blocking occurs

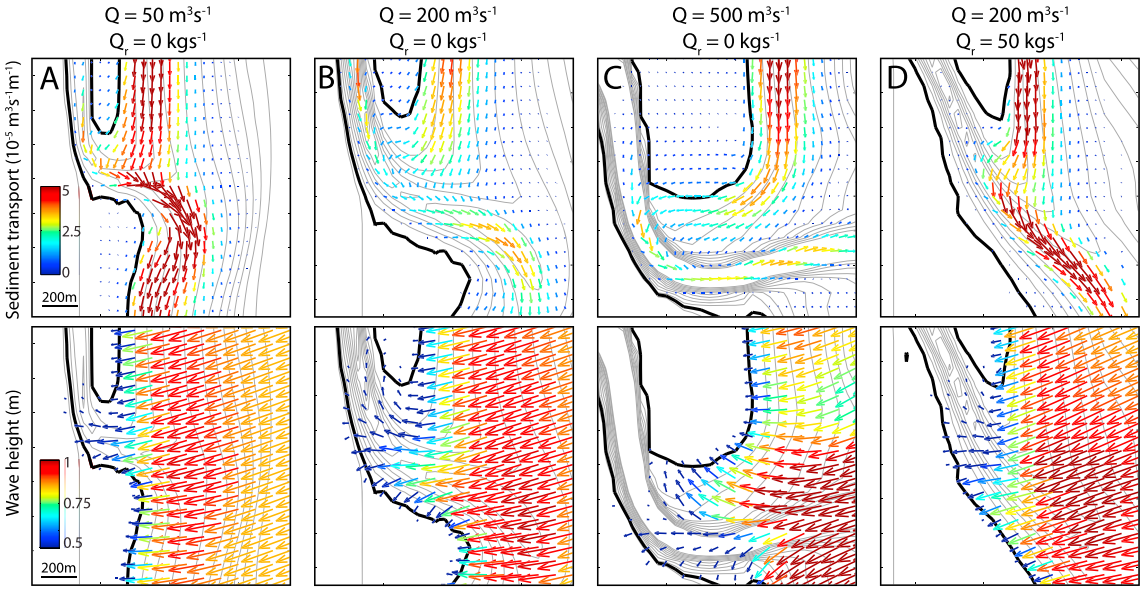

Figure 6. Sediment transport fluxes and wave height for close-ups of the four cases shown in Figure 4. (Figures 6a–6d, top) Sediment transport direction and magnitude only of the updrift sediment. (bottom) Significant wave height and direction showing how the wave field interacts with the river mouth morphology and the river jet. Grey lines show the bathymetry contours up to 5 m of water depth, black line is 0 m.

because the river mouth bar and river mouth jet affect the incoming waves; waves refract into the river mouth bar and into the river mouth jet, creating a zone of relatively low wave heights and therefore low alongshore transport updrift of the river mouth (Figures 6b and 7b). This process favors updrift sediment deposition, driving spit formation and river mouth migration.

With even larger fluvial discharge (Figures 4c and 6c), updrift sediment is sequestered via the channel in the river mouth bar at about 3 m water depth. In these simulations, the river mouth jet is unsteady, regularly changing its path around the river mouth bar. When the jet is directed updrift around the river mouth bar, continued sediment deposition tends to force the jet downdrift (and vice versa). The strong jet affects the incoming waves, limiting bypassing. Bypassing occurs via the channel through the formation and migration of river mouth bars (Figures 4c and 6c, see also Animation S3). In this case, the river mouth spit consists of both sediment eroded by the channel from the downdrift bank of the river mouth and of updrift sediment transported along the spit and through the channel. As the river mouth migrates downdrift, part of the river mouth bar merges back onshore, updrift of the river mouth.

With a significant fluvial sediment flux, the river mouth is net progradational (Figure 6d, see also Animation S4). Bypassing occurs via the channel, and the river mouth jet is strongly deflected to set up a regime where wave height does not vary alongshore (similar to Figure 6a). There is no zone of low wave heights updrift of the river mouth that would result in sediment deposition.

6.2. Contrasting River Mouth Bar Versus Jet Effects on Bypassing

In the previous section, we identified refraction of waves away from the updrift coast as the dominant mechanism for updrift sediment deposition, spit formation, and river mouth migration. Refraction of waves away from the updrift coast can be either due to current refraction of the waves in the presence of the river mouth jet or due to depth-refraction of the waves in the presence of a river mouth bar. To explore the relative importance of depth refraction versus current refraction, we investigated wave heights and directions in three model experiments: (1) a river mouth with a river mouth jet, but prior to any morphological change (Figure 7a), (2) our typical experiment with a river mouth jet and a fully developed morphology (Figure 7b), and (3) an experiment without a river mouth jet, but with the developed morphology of the second experiment (Figure 7c).

Our model experiments suggest that, similar to conclusions drawn recently by *Olabarrieta et al.* [2014] and *Chen et al.* [2015], the majority of the wave refraction around our simulated river mouth is driven by the presence of the river mouth bar (Figure 7b). We do not find a significant difference in the wave heights with

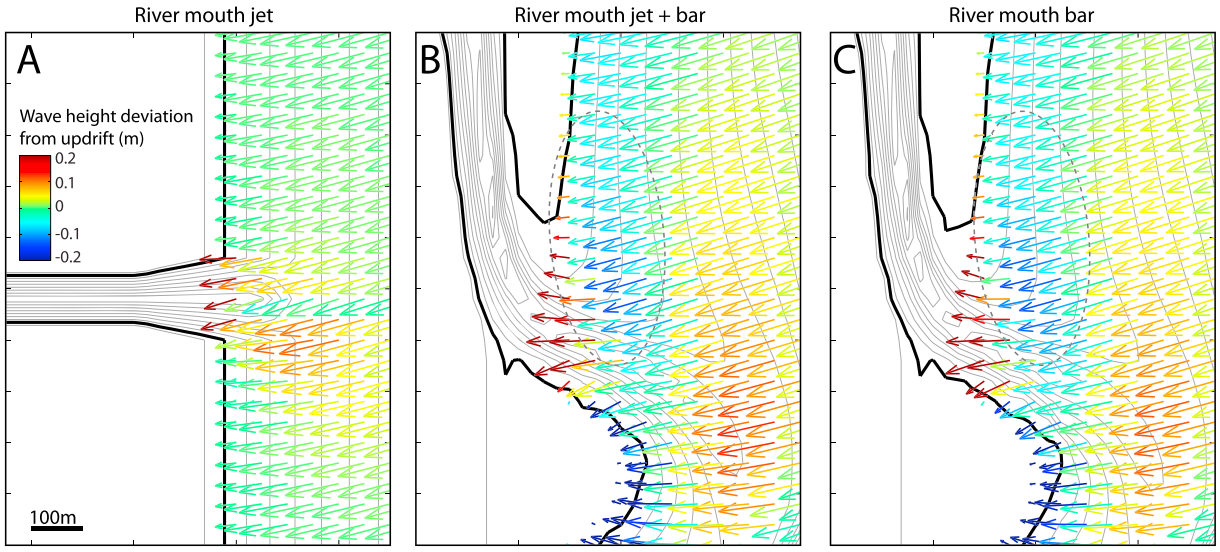

Figure 7. Wave height deviations in the presence of (a) the river mouth jet (after the model hydrodynamic spin-up and before any simulated morphological change), (b) the river mouth jet and bar (after 3.2 years of morphodynamic change), and (c) the river mouth bar (after 3.2 years of morphodynamic change with added 24 h of hydrodynamic spin-up without fluvial discharge). Vector length and direction represent the wave field; vector color represents the wave height deviation from a cross-shore profile updrift that is unaffected by the river mouth. Grey lines show the bathymetry contours up to 5 m of water depth; black line is 0 m. $Q = 200\ m^3\ s^{-1}$, $H_s = 1$ m. Dashed ellipse in Figures 7b and 7c show the region of lower wave heights updrift of the river mouth responsible for sediment deposition and spit growth.

or without a river mouth jet (compare Figure 7b to Figure 7c). Note however that these findings are dependent on the accuracy of SWAN in these shallow and energetic environments.

6.3. Wave and River Mouth Controls on Bypassing

To expand on the descriptive findings above, we sought a nondimensional parameter that would best predict alongshore sediment transport bypassing for river mouths. We ran model experiments with fluvial water discharge ranging from $50\ m^3\ s^{-1}$ to $1000\ m^3\ s^{-1}$ and wave heights ranging from 0.7 m to 1.5 m (See supporting information Table S2 for an overview of the model experiments). As discussed in section 6.1, interactions between the jet, the river mouth bar, and the waves, and in particular the jet deflection by the waves, strongly influence the pathways of alongshore sediment bypassing. To characterize jet deflection, we look to the ratio of the jet momentum flux versus the alongshore component of the wave momentum flux,

$$\frac{M_J}{M_W} = \frac{\rho_w \cdot Q \cdot u}{S_{xy} \cdot W} = \frac{\rho_w \cdot Q \cdot u}{E \cdot n(\cos\theta \cdot \sin\theta) \cdot W}, \tag{4}$$

where M_J is the momentum flux of the jet at the river mouth ($kg\ m\ s^{-2}$), M_W is the wave momentum flux ($kg\ m\ s^{-2}$), ρ_w is the water density ($kg\ m^3$), Q is the river discharge ($m^3\ s^{-1}$), u is the depth- and width-averaged river velocity ($m\ s^{-1}$), S_{xy} is the alongshore-directed component of the radiation stress ($N\ m^{-1}$), W is the width of the river mouth (m), E is the wave energy density ($N\ m^{-1}$) which equals $\frac{1}{16} \cdot \rho_w \cdot g \cdot {H_s}^2$ [*Airy*, 1841], g is the vertical acceleration due to gravity ($m\ s^{-2}$), H_s is the significant wave height (m), n is the ratio of the group velocity to phase velocity of the incoming (deep water) waves, and θ is the incoming wave angle. We choose the deep water wave formulation of the radiation stress to form a straightforward relation between the model boundary conditions and the computed wave momentum flux.

To avoid complications arising from shoreline reorientation, we investigate experiments without fluvial sediment supply to determine whether this balance (equation (4)) can characterize jet deflection. Model results suggest that when the momentum flux balance exceeds approximately 0.5 (i.e., for relatively stronger fluvial momentum flux), the river mouth shifts from a stable deflected jet to a morphologically unstable jet (Figure 8a). Note that the jet is not hydrodynamically unstable (as in *Canestrelli et al.* [2014]) but morphologically unstable. The unstable river mouth jet switches its orientation between deflected away from the waves (positive angle) and into the waves (negative angle, Figure 8a) because of the formation and migration of the river mouth bar (Figure 4c, and Animation S3).

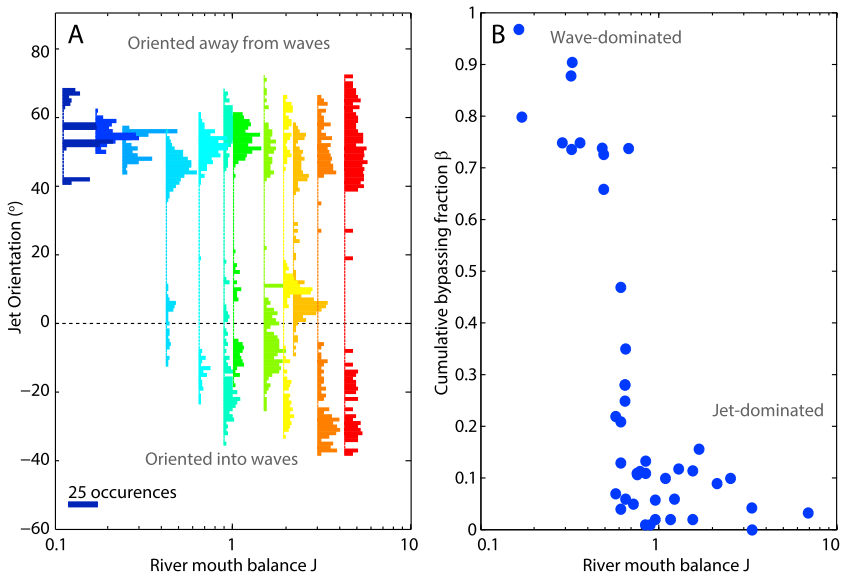

Figure 8. (a) Histograms of jet orientation for 12 model experiments with different river mouth balance ratios J (equation (4)) and no fluvial sediment supply. Colors are used to visually distinguish the model experiments. +90° is shore-parallel away from the waves, 0° is shore-normal, and −90° is shore-parallel into the wave approach direction. The jet orientation is computed at the offshore location of the maximum cross-shore velocity. (b) Average alongshore sediment bypassing fraction β for all model experiments at different river mouth balance ratios J (equation (5)).

6.4. Fluvial Sediment Supply Controls on Bypassing

As shown in section 6.1, fluvial sediment supply significantly affects alongshore sediment bypassing. To quantify this phenomenon, we ran 45 experiments with discharge varying between 50 $m^3 s^{-1}$ and 1000 $m^3 s^{-1}$ and fluvial sand supply ranging from 0 $kg s^{-1}$ to 100 $kg s^{-1}$. For river mouths along a straight coastline, the alongshore sediment transport far updrift and far downdrift of the river mouth are approximately equal. By supplying fluvial sediment to the downdrift coastline, littoral sediment from updrift can no longer be transported along the downdrift coastline and will therefore not be bypassed. To account for the decrease in bypassing due to fluvial sediment supply, we include in the momentum flux balance (equation (4)) a nondimensional sediment flux balance $Q_s/(Q_s+Q_r)$, where Q_s is the alongshore sediment transport flux ($m^3 s^{-1}$) and Q_r is the fluvial sediment flux ($m^3 s^{-1}$). Combined, we formulate the nondimensional river mouth balance J,

$$J = \frac{M_J}{M_W} \cdot \frac{Q_s}{Q_s + Q_r}. \tag{5}$$

We find that the river mouth balance J is able to explain the observed variability in long-term (cumulative) alongshore sediment bypassing fraction β (Figure 8b). Alongshore sediment bypassing appears bimodal, with the majority of model experiments tending toward either uninterrupted bypassing of littoral sediment ($\beta \rightarrow 1$) or complete blocking ($\beta \rightarrow 0$). When the wave momentum flux exceeds the jet momentum flux, the river mouth is wave-dominated ($J << ½$) and bypassing is high ($\beta > 0.5$). Waves limit the size of the river mouth bar and deflect the river mouth jet, such that there is a small effect updrift wave refraction effect limiting updrift wave height. When, on the other hand, the jet momentum flux is high, the river mouth is jet-dominated ($J >> ½$) and alongshore sediment is not able to bypass the river mouth (Figure 8b). The river mouth bar and the river mouth jet effectively cause the updrift waves to refract, away from the river mouth spit, and cause deposition. Interestingly, this framework suggests that, by increasing alongshore sediment bypassing, increases in the fluvial sediment flux make the river mouth more wave-dominated.

7. River Mouth Migration

7.1. Dimensions of the River Mouth Spit

Using our understanding of river mouth bypassing from our model experiments, we can estimate the alongshore migration rate of both simulated and natural river mouths. If bypassing is limited, the rate of river mouth

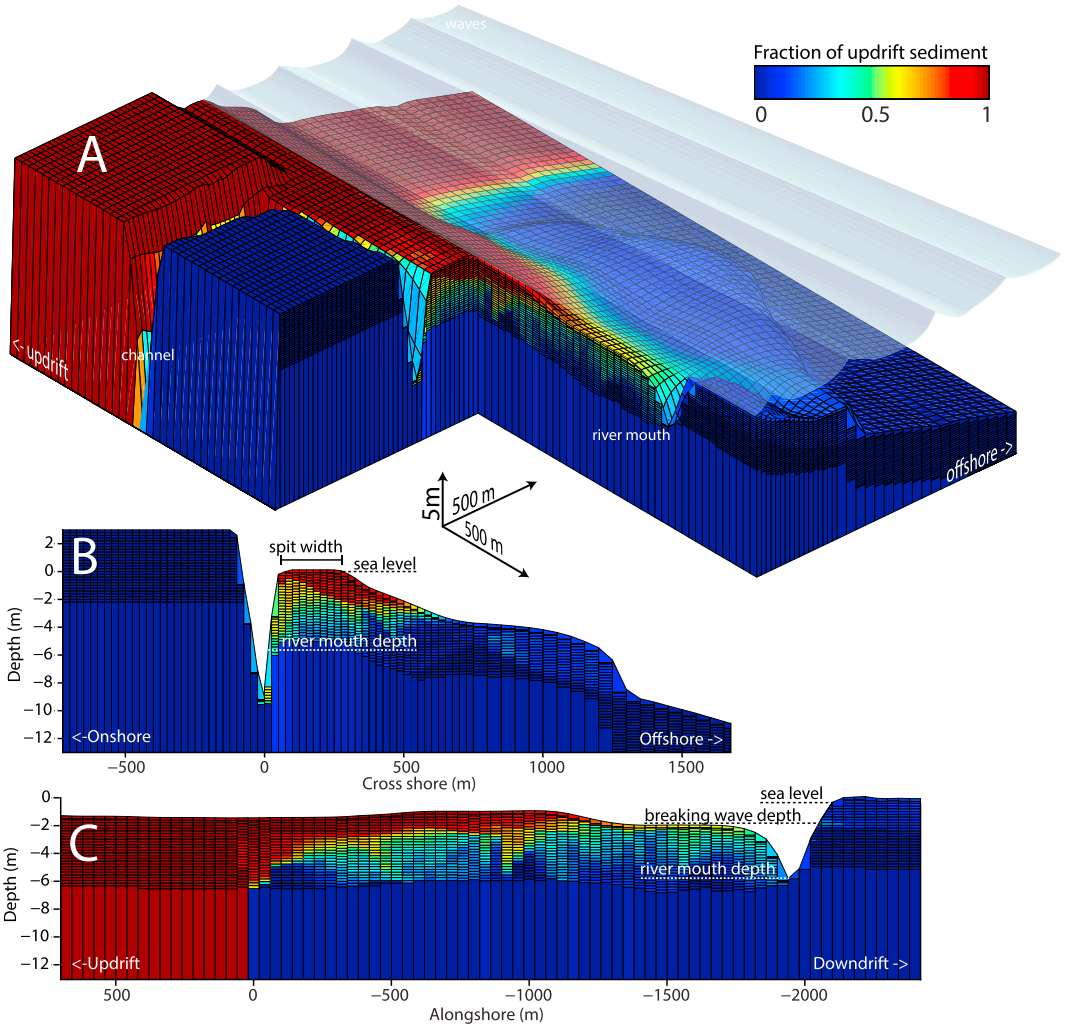

Figure 9. Morphology and depth slices of the river mouth spit colored by the fraction of updrift sediment. (a) View looking offshore and updrift, shaded waves indicate sea level, (b) cross section of the river mouth spit, (c) long section of the river mouth spit. Note that the lighter shaded blue bars extending below the channel depth arise from limited vertical resolution of the bed composition tracking at depth.

migration should be controlled by the volume of blocked updrift sediment divided by the representative cross-sectional area of the river mouth spit A_b (equation (1)). Thus, for successful prediction of river mouth migration rates or for bypassing estimates of natural systems based on observed migration rates, we need to know the cross-sectional area of the river mouth spit composed of updrift sediment (A_b).

Investigating the origin of sediments incorporated in our modeled river mouth spits, we find that the river mouth spit only partially consist of updrift sediment (Figure 9c). Rather, a significant fraction of spit deposits are composed of eroded sediment from the downdrift beach (Figure 9). As the downdrift sediment is eroded and transported onto the river mouth bar, subsequent migration of the river mouth downdrift of the bar leads to onshore sediment movement and incorporation of the downdrift sediment into the spit (Figure 9c). Using the model experiments for different fluvial discharges and different offshore wave heights, we find that approximately one half of the thickness of the river mouth spit is composed of updrift sediment (Figure 10a).

Because littoral transport far updrift and far downdrift of the river mouth along a straight shoreline are equal (i.e. 1 Q_s) and $\beta \cdot Q_s$ is bypassed, the volume of eroded downdrift sediment transported along the downdrift coastline in steady state is $(1-\beta) \cdot Q_s$. Because we find that the river mouth spit is composed of approximately 50% updrift sediments, which accumulate at a rate of $(1-\beta) \cdot Q_s$, downdrift sediments are also accumulating at a rate of $(1-\beta) \cdot Q_s$ in the river mouth spit.

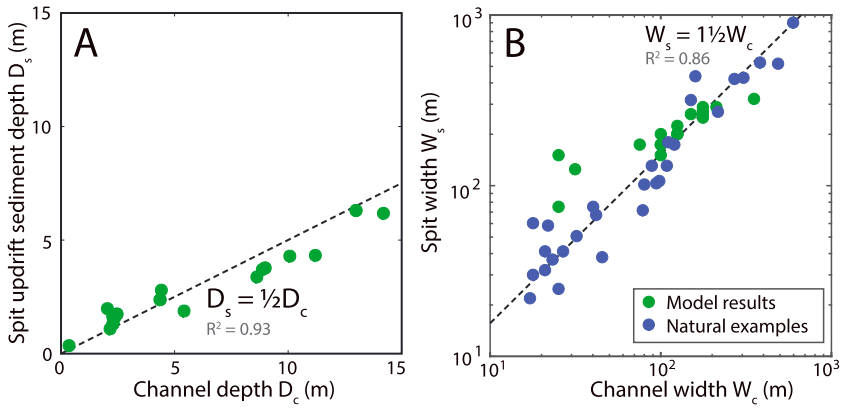

Figure 10. (a) Average thickness, D_s, of modeled updrift sediment in the river mouth spit for different channel depths D_c. (b) Average spit width, W_s, for different channel widths, W_c, for both model results (green), and natural examples (blue). Dashed line indicates an approximate fit to model results and natural examples. See supporting information Table S3 for a list of the natural examples.

Additionally, our model experiments and a selection of natural examples indicate that the channel width (W_c) is a good predictor of the width of the river mouth spit (W_s, Figure 10b). Across 2 orders of magnitude in channel size, river mouth spit width is about 1½ times the channel width. We note here that the process of river mouth spit formation could be analogous to the processes that control the curvature in meandering rivers. As a migrating river mouth bends approximately 90° to become perpendicular to the shoreface (e.g., Figure 3c), the width of the river mouth spit plus half of the channel width is equal to its meander curvature radius. The observed scaling between river mouth spit width and channel width of 1½ (Figure 10b) therefore corresponds to a dimensionless ratio of meander curvature radius to channel width of 2, commonly found in river meanders [*Leopold and Wolman*, 1960] and associated with a maximum in meander bend migration rates [*Hickin and Nanson*, 1984]. However, note that we do not include secondary flow in our depth-averaged flow model experiments. River mouth migration in our model is forced by "bar push" deposition of littoral sediment and "bank pull" erosion caused by fluvial currents.

7.2. Predictive Model of River Mouth Migration

The combination of alongshore bypassing fractions (β), spit updrift sediment depth (D_s), and spit width (W_s) allows us to develop a predictive model of river mouth migration, building on the mass balance proposed earlier (equation (1)). First, we estimate the cumulative alongshore sediment bypassing fraction β as a function of the river mouth balance J (equation (5)) by fitting a smooth sigmoid shape β (J) to the bypassing data,

$$\beta(J) = \frac{1}{1 + a \cdot J^b}, \tag{6}$$

with fitted parameters $a = 10$ and $b = 3$ (Figure 11a). This functional form ensures that β (J) is smooth and that bypassing in the wave-dominated limit ($J \to 0$) approaches 1, and bypassing for jet-dominated river mouths ($J \to \infty$) tends toward 0.

Second, the representative spit cross-sectional area A_b (m^2) is the product of spit width W_s (m) and the spit updrift sediment depth D_s (m) (Figure 1). Following the dependence of spit width to channel width and spit updrift sediment thickness to channel depth established earlier (Figure 10), we can formulate a predictive model for the river mouth migration rate v, as

$$v = \frac{Q_s \cdot [1 - \beta]}{A_b} = \frac{Q_s \cdot [1 - \beta(J)]}{\frac{3}{2} W_c \cdot \frac{1}{2} D_c}, \tag{7}$$

which allows us to estimate the migration rate for a given river mouth depending on the river mouth balance J. Reorganized, this also allows us to estimate the bypassing fraction β using the observed migration rate of a particular river mouth:

$$\beta = 1 - \left(\frac{v \cdot \frac{3}{2} W_c \cdot \frac{1}{2} D_c}{Q_s} \right). \tag{8}$$

These relationships can be tested using both modeled and natural examples.

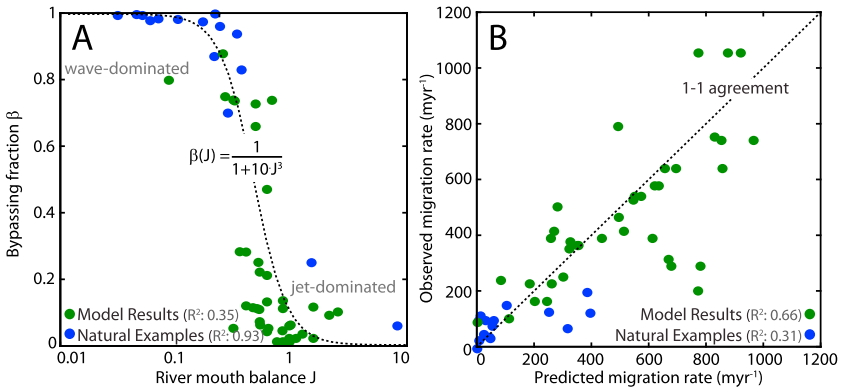

Figure 11. (a) Alongshore sediment bypassing for model results and natural examples. The dotted line shows the fit of a simple logistic function (equation (6)) that relates bypassing to the river mouth balance *J* (defined in equation (5)). (b) Predicted versus observed migration rates for our model results and natural examples.

8. Application to Natural Examples

The simple boundary conditions and idealized domain used in our model runs allow us to generalize the model findings and to apply them to wide range of natural systems. We analyzed 15 natural river mouths distributed across the world (i.e., in Georgia, Nicaragua, Honduras, Brazil, and Senegal) to investigate their bypassing fractions and alongshore migration rates, limiting our analysis to cases without significant fluvial sediment supply and without significant tidal range.

We calculated migration rates for these river mouths using satellite imagery from Google Earth or NASA Landsat, tracking the river mouth location across multiple images spanning at least 2 years. For all river mouths except the Senegal River, we estimated discharge and channel depth based on hydraulic geometry [*Andren*, 1994] using the average channel width upstream of the river mouth. In all cases, alongshore sediment transport was estimated with the CERC formula, cast in deep water wave terms, assuming shore-parallel depth contours and a CERC coefficient *K* of 0.15 [*Komar*, 1971; *Nienhuis et al.*, 2015b]. According to laboratory experiments by *Kamphuis* [1991], the CERC equation overestimates alongshore sediment transport for steep beaches, which could indicate a negative dependence of the coefficient *K* on beach slope. We do not take into account the beach slope in our estimates of alongshore sediment transport. Using the WaveWatch III reanalysis hindcast [*Chawla et al.*, 2013], we retrieved directional deep water wave time series from 1979 to 2009 to estimate the long-term wave climate. See supporting information Table S3 for an overview of the natural examples.

The observed migration rate of the natural river mouths constrains the fraction of alongshore sediment transport that is able to bypass the river mouth. Given the approximations in the analysis, we observe a surprisingly good fit between inferred bypassing fraction (equation (8)) and the river mouth balance *J* (Figure 11a). Next, we use the bypassing function β (*J*) equation (6)) with the calculated river mouth balance *J* to predict a migration rate for the model results (Figure 11b, green markers) and the natural examples (Figure 11b, blue markers). Note that the deviations of the model results away from the 1-1 agreement are due to the approximations in the bypassing function (equation (6)) and the representative river mouth spit cross-sectional area, A_b. For river mouths with high bypassing, a small relative error in the estimated bypassing fraction β results in a large relative error in the calculated migration rate ($v \sim 1\text{-}\beta$). This caused the fit of the natural examples to deteriorate compared the model experiments (Figure 11b).

9. River Mouth Spit Breaching

For rapidly migrating river mouths, alongshore migration is often stopped by a breach in the spit, typically thought to be initiated by either increased water level setup in the channel due to floods or from the coast due to storms or tides [*Cooper*, 1990]. Investigating a model experiment over 14 morphological years, we find that even under constant forcing conditions, the modeled system can undergo repeated cycles of spit elongation interrupted by distinct breaching events (Figure 12a and Animation S5). In this model experiment (Table S2 #46), breaches initiate when the river mouth has migrated approximately 2500 m from the original

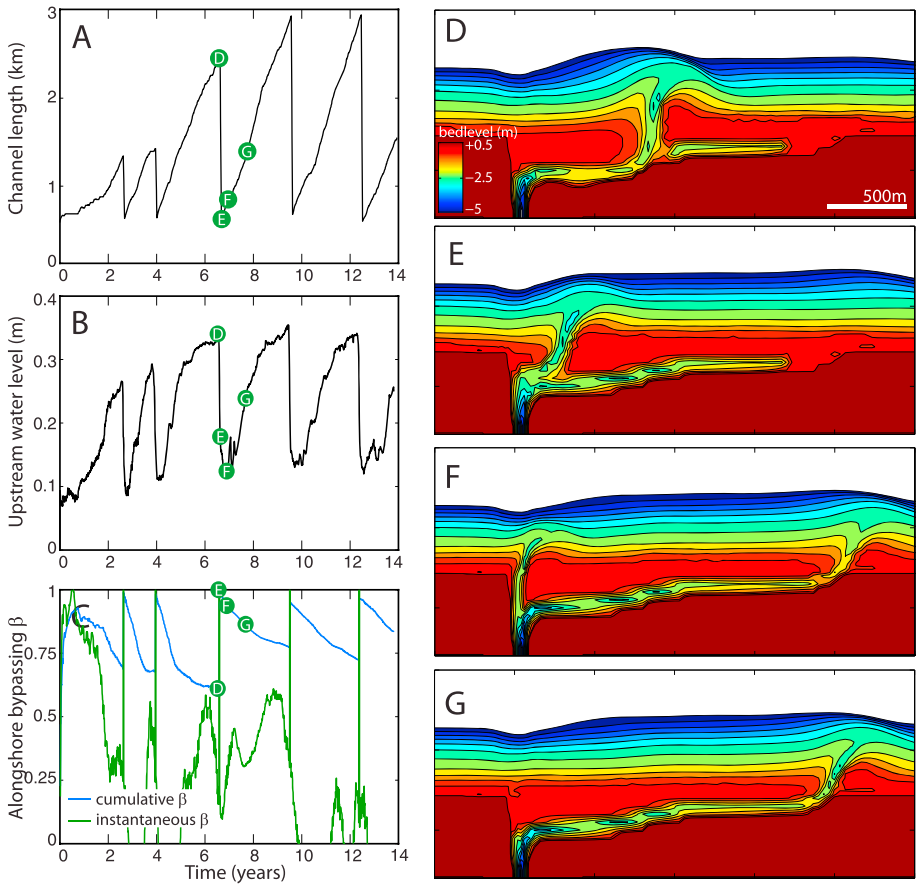

Figure 12. Example of a river mouth spit breach. (a) The channel length, (b) water level, and (c) alongshore sediment bypassing over the course of 14 model years. Green markers show the times of the four model snapshots in Figures 12d–12g. (d–g) Close-up of the river mouth morphology at times indicated in the plots to the left. Colors indicate bed level relative to mean sea level (m).

river location, when the upstream water level reaches a critical threshold of approximately 30 cm (Figure 12 b). After about 5 years of morphological spin-up, breaches occur at a regular time interval and at a similar channel length (Figure 12a). As the river mouth migrates and the channel maintains a constant water surface slope, the elevation of the water surface at the upstream boundary is directly related to the channel length. Therefore, when the channel length reaches a critical length (corresponding to an elevated water level of 30 cm) superelevation in the channel initiates a breach (Animation S5).

We can use equation (1) to evaluate the controls on river mouth spit breaching timescales. Here $T_{\text{breach}} = L_{\text{breach}}/v$, where T_{breach} is the breaching timescale (s), L_{breach} is the breaching length scale (m) and v is the alongshore migration rate of the river mouth (m s^{-1}). Investigating bypassing through time, we find that each breaching event is associated with a peak in the instantaneous alongshore sediment bypassing fraction β (Figure 12c). Therefore, in order to successfully relate the breaching length scale to a breaching timescale, the key bypassing fraction is the cumulative bypassing fraction during the migration phase of the river mouth just before a breach occurs (in this case $\beta_{\text{cum}} \approx 0.7$, Figure 12c).

Combining the bypassing estimate with the breaching length scale to obtain the breaching time scale, we arrive at

$$T_{\text{breach}} = \frac{L_{\text{breach}}}{v} = \frac{L_{\text{breach}} \cdot A_b}{Q_s(1-\beta)}, \tag{9}$$

which for $L_{\text{breach}} = 2500$ m, $\beta = 0.7$, $Q_s = 0.012$ m^3 s^{-1}, and $A_b = 250$ m^2 (Table S2, 46) leads to a breaching interval of 2.4 years, closely matching the modeled channel dynamics. This breaching experiment (Figure 12) also

indicates that migration does not continue perpetually and that without the river mouth progradation associated with fluvial sediment supply, bypassing averaged over long timescales will always tend to 1.

10. Discussion

10.1. Alongshore Migration Rate

In this study, we have formulated a predictive relationship for the alongshore migration rate of river mouth spits. Migration generally ranges between zero and several hundred meters per simulation year and is controlled by the cross-sectional area of the river mouth spit and by the volume of alongshore sediment transport that is not bypassed. Obliquely approaching waves that deflect the river mouth jet and limit the size of the river mouth bar control the pathways and rates of alongshore sediment bypassing (Figure 6). We estimate jet deflection, and therefore alongshore sediment bypassing, with the ratio of jet momentum flux versus the alongshore-directed component of the wave momentum flux (Figure 8). Investigating model experiments and natural examples, we found that the cross-sectional area of the spit increases with increasing channel size (Figure 10). Because the fraction of alongshore sediment transport that is blocked also increases for increasing channel size, the combined effect is that the river mouth migration rate is maximized for intermediate-sized river mouths (Figure 5).

10.2. Short-Term and Long-Term Fluctuations

The model experiments shown here with constant boundary conditions are a significant simplification from the complicated marine and fluvial processes that affect river mouths. River mouths change seasonally and are influenced by extreme events, such as storms or floods [e.g., *Cooper*, 1990; *Hart*, 2007]. However, the results reported here hint that the dynamics of channel bypassing, migration, and breaching can be sustained even with constant forcing, i.e., in the absence of punctuated events of high intensity. Even though storms and floods most likely dictate the short-term dynamics of small river mouth systems, extreme events are not necessary ingredients to gain process understanding of long-term river mouth morphodynamics.

The effect of fluvial and wave-climate fluctuations on river mouth dynamics can be assessed by their formative timescales. For fluvial geomorphology, the formative timescale is typically the bankfull, 1½ year flood [*Wolman and Miller*, 1960]. The analysis of *Kirk* [1991] showed that some river mouth spits breach at these timescales. *Kraus et al.* [2002] found that storm-induced breach timescales correlate with the 10 year storm surge height relative to the tidal range, a proxy for the subaerial elevation of the river mouth spit. Alongshore sediment transport, the main mechanism for bypassing and migration, acts on much shorter timescales [*Hicks and Inman*, 1987], leading to river mouth migration (low bypassing) or closure (high bypassing) to be associated with average day-to-day conditions [*Hicks and Inman*, 1987; *Kirk*, 1991]. However, while the formative timescale for alongshore sediment transport is short, the direction of alongshore sediment transport can be strongly seasonal. The multiannual migration rate and direction of river mouths therefore can potentially be dependent not just on the annual average bypassing conditions but on the degree of temporal overlap of the directional wave climate with the average fluvial discharge.

Fluvial floods deliver coarse sediment and often lead to the formation of ephemeral mouth bars in wave-dominated environments. These mouth bars can decrease alongshore sediment transport on short timescales but, on seasonal timescales, can feed the littoral system or be transported offshore [*Warrick and Barnard*, 2012]. Fluvial sediment can also form offshore platforms topped by emergent barrier islands that increase alongshore sediment bypassing [*Giosan*, 2007; *Giosan et al.*, 2013]. While the parameterizations presented here are useful for studies of deltaic and coastline evolution on larger scales [*Nienhuis*, 2016], future work will be required to study the longer timescale effect of fluvial sediment on alongshore sediment bypassing. Similarly, the effect of tides on both the modulation of sediment discharge [e.g., *Leonardi et al.*, 2013, 2015], and waves should be addressed in future studies.

10.3. Erosion of the Downdrift Coast

The link between river mouth migration, alongshore sediment transport, and river mouth bypassing established here relies in part on the ability of the river mouth to freely erode into the downdrift coastline. However, the migration of natural river mouths is in many cases limited by the strength of the downdrift bank [*Izumi et al.*, 1999; *Cooper*, 2001]. Future studies will be focused on the mechanisms with which sediment is eroded from the downdrift bank and how this sediment is either incorporated into the spit or transported

downdrift. Additionally, because the strength of the downdrift bank should have a direct effect on the channel migration rate, future studies could include a downdrift lithology factor such that not just the river mouth balance J (equation (5)), but also sediment erodibility will influence bypassing.

11. Conclusions

This study has provided quantitative understanding of river mouth morphodynamics in wave-dominated environments. Our findings are not only relevant for the longer timescale evolution and storage of terrestrial signals in the marine environment, but, because river mouths and adjacent coasts experience changes of many kilometers on human timescales, this quantitative understanding of river mouth behavior can be applied to coastal planning and management problems. Furthermore, the predictive framework of bypassing and channel migration can be used to analyze how river mouths influence the dynamics of larger wave-influenced deltaic systems and offer insight into the future evolution of river mouths under anthropogenic modifications and climate change.

Using model experiments and natural examples, we found that the fraction of alongshore sediment that is bypassed and the size of the river mouth spit controls the alongshore migration rate of river mouths. Alongshore bypassing pathways and bypassing fluxes are themselves controlled by river mouth jet deflection. For a downdrift-deflected jet, updrift alongshore sediment transport is not affected by the river mouth; the resulting sediment bypassing fraction is high, and bypassing can occur close to the shoreline. If the jet is not deflected, wave-current refraction and wave-depth refraction form a zone of low alongshore transport updrift of the river mouth, effectively disabling alongshore sediment bypassing. We found in our model experiments that bypassing can be predicted by the ratio of jet momentum flux versus the alongshore component of the wave momentum flux. The coupling between alongshore sediment bypassing and river mouth migration has enabled us to formulate a predictive framework of alongshore sediment bypassing that can be tested on natural examples. Furthermore, model experiments show that river mouth migration, bypassing, and spit breaching dynamics can arise even under constant discharge and wave conditions, potentially setting up an important autogenic clock for wave-dominated river mouths. Future studies will be focused on how temporal fluctuations of fluvial sediment supply and wave directionality affect bypassing and fluvial sediment distribution within the coastal zone.

Acknowledgments

This research was supported by NSF grant EAR-0952146 to Andrew Ashton and Liviu Giosan and a GSA Student Research Grant to Jaap Nienhuis. We thank Jeff List for sharing his Delft3D setup. The data for this paper are available upon request from the authors. This manuscript benefitted from constructive comments from Jon Warrick, two anonymous reviewers, the Associate Editor, and the Editor.

References

Aibulatov, N. A., and I. F. Shadrin (1961), Some data on the long-shore drift of sand near natural obstacles, *Tr. Inst. Okeanol. Akad. Nauk. SSSR*, *53*.

Airy, G. B. (1841), Tides and waves, *Encycl. Metrop.*, *3*, 396.

Andren, H. (1994), Development of the Laitaure delta, Swedish Lapland: A study of growth, distributary forms, and processes, Uppsala University.

Anthony, E. J. (2015), Wave influence in the construction, shaping and destruction of river deltas: A review, *Mar. Geol.*, *361*, 53–78, doi:10.1016/j.margeo.2014.12.004.

Ashton, A. D., and L. Giosan (2011), Wave-angle control of delta evolution, *Geophys. Res. Lett.*, *38*, L13405, doi:10.1029/2011GL047630.

Bakker, W. T. J. N. P., and T. Edelman (1964), The coastline of river-deltas, in *Proc. of the 9th Conf. on Coastal Engineering*, edited by B. Edge, pp. 199–218, ASCE, Lisbon.

Balouin, Y., P. Ciavola, and D. Michel (2006), Support of subtidal tracer studies to quantify the complex morphodynamics of a river outlet: The Bevano, NE Italy, *J. Coast. Res.*, *1*(39), 602–606.

Bates, C. C. (1953), Rational theory of delta formation, *Am. Assoc. Pet. Geol. Bull.*, *37*(9), 2119–2162.

Bhattacharya, J. P., and L. Giosan (2003), Wave-influenced deltas: Gseomorphological implications for facies reconstuction, *Sedimentology*, *50*(1), 187–210, doi:10.1046/j.1365-3091.2003.00545.x.

Booij, N., R. C. Ris, and L. H. Holthuijsen (1999), A third-generation wave model for coastal regions: 1. Model description and validation, *J. Geophys. Res.*, *104*(C4), 7649–7666, doi:10.1029/98JC02622.

Boyd, R., R. Dalrymple, and B. A. Zaitlin (1992), Classification of clastic coastal depositional environments, *Sediment. Geol.*, *80*(3–4), 139–150, doi:10.1016/0037-0738(92)90037-R.

Brocatus, J. (2008), Sediment budget analysis of the Santa Barbara littoral cell, Delft University of Technology.

Bruun, P., and F. Gerritsen (1959), Natural by-passing of sand at coastal inlets, *J. Waterw. Harb. Div.*, *85*(4), 75–107.

Canestrelli, A., W. Nardin, D. Edmonds, S. Fagherazzi, and R. Slingerland (2014), Importance of frictional effects and jet instability on the morphodynamics of river mouth bars and levees, *J. Geophys. Res. Oceans*, *119*, 509–522, doi:10.1002/2013JC009312.

Chawla, A., D. M. Spindler, and H. L. Tolman (2013), Validation of a thirty year wave hindcast using the Climate Forecast System Reanalysis winds, *Ocean Model.*, *70*, 189–206, doi:10.1016/j.ocemod.2012.07.005.

Chen, J.-L., T.-J. Hsu, F. Shi, B. Raubenheimer, and S. Elgar (2015), Hydrodynamic and sediment transport modeling of New River Inlet (NC) under the interaction of tides and waves, *J. Geophys. Res. Oceans*, *120*, 4028–4047, doi:10.1002/2014JC010425.

Cooper, J. A. G. (1990), Ephemeral stream-mouth bars at flood-breach river mouths on a wave-dominated coast: Comparison with ebb-tidal deltas at barrier inlets, *Mar. Geol.*, *95*(1), 57–70, doi:10.1016/0025-3227(90)90021-B.

Cooper, J. A. G. (2001), Geomorphological variability among microtidal estuaries from the wave-dominated South African coast, *Geomorphology*, *40*(1–2), 99–122, doi:10.1016/S0169-555X(01)00039-3.

Correggiari, A., A. Cattaneo, and F. Trincardi (2005), The modern Po Delta system: Lobe switching and asymmetric prodelta growth, *Mar. Geol.*, *222*, 49–74, doi:10.1016/j.margeo.2005.06.039.

Dean, R. G. (1991), Equilibrium beach profiles: Characteristics and applications, *J. Coast. Res.*, *7*(1), 53–84.
Deltares (2014), *User Manual Delft3D*, Deltares, Delft, The Netherlands.
Dodet, G., X. Bertin, N. Bruneau, A. B. Fortunato, A. Nahon, and A. Roland (2013), Wave-current interactions in a wave-dominated tidal inlet, *J. Geophys. Res. Oceans*, *118*, 1587–1605, doi:10.1002/jgrc.20146.
Dominguez, J. M. L. (1996), The Sao Francisco strandplain: A paradigm for wave-dominated deltas?, *Geol. Soc. Lond. Spec. Publ.*, *117*(1), 217–231, doi:10.1144/GSL.SP.1996.117.01.13.
Edmonds, D. A., and R. L. Slingerland (2007), Mechanics of river mouth bar formation: Implications for the morphodynamics of delta distributary networks, *J. Geophys. Res.*, *112*, F02034, doi:10.1029/2006JF000574.
Fagherazzi, S., D. A. Edmonds, W. Nardin, N. Leonardi, A. Canestrelli, F. Falcini, D. J. Jerolmack, G. Mariotti, J. C. Rowland, and R. L. Slingerland (2015), Dynamics of river mouth deposits, *Rev. Geophys.*, *69*, 1–31, doi:10.1002/2014RG000451.
Falcini, F., A. Piliouras, R. Garra, A. Guerin, D. J. Jerolmack, J. Rowland, and C. Paola (2014), Hydrodynamic and suspended sediment transport controls on river mouth morphology, *J. Geophys. Res. Earth Surf.*, *119*, 1–11, doi:10.1002/2013JF002831.
Fitzgerald, D. M. (1982), Sediment Bypassing at Mixed Energy Tidal Inlets, in *Proceedings of 18th Conference of Coastal Engineering, Vol. 18*, edited by B. L. Edge, pp. 1094–1118, ASCE, Cape Town, South Africa.
Friedman, G. M. (1967), Dynamic processes and statistical parameters compared for size frequency distribution of beach and river sands, *J. Sediment. Res.*, *37*(2), 327–354, doi:10.1306/74D716CC-2B21-11D7-8648000102C1865D.
Gelfenbaum, G., A. W. Stevens, I. Miller, J. A. Warrick, A. S. Ogston, and E. Eidam (2015), Large-scale dam removal on the Elwha River, Washington, USA: Coastal geomorphic change, *Geomorphology*, *246*, 649–668, doi:10.1016/j.geomorph.2015.01.002.
Giosan, L. (1998), Long term sediment dynamics of Danube delta coast, in *Physics of Estuaries and Coastal Seas*, edited by J. Dronkers and M. Scheffers, pp. 365–376, Balkema, Rotterdam.
Giosan, L. (2007), Morphodynamic feedbacks on deltaic coasts: Lessons from the wave-dominated Danube Delta, in *Coastal Sediments '07*, edited by N. C. Kraus and J. D. Rosati, pp. 828–841, doi:10.1061/40926(239)63.
Giosan, L., J. P. Donnelly, E. Vespremeanu, J. P. Bhattacharya, C. Olariu, and F. S. Buonaiuto (2005), River delta morphodynamics: Examples from the Danube Delta, in *River Deltas: Concepts, Models and Examples*, edited by L. Giosan and J. P. Bhattacharya, SEPM, Tulsa, Okla.
Giosan, L., S. Constantinescu, F. Filip, and B. Deng (2013), Maintenance of large deltas through channelization: Nature vs. humans in the Danube delta, *Anthropocene*, *1*, 35–45, doi:10.1016/j.ancene.2013.09.001.
Grijm, W. (1960), Theoretical forms of shorelines, in *7th Conference on Coastal Engineering*, vol. 2, edited by B. Edge, pp. 197–202, ASCE, Lisbon.
Guilchar, A., and J. P. Nicholas (1954), Observation sur la Langue de Barbarie et les bras du Senegal aux environs de Saint-Louis, *Bull. Inf. C.O.E.C.*, *6*, 227–242.
Hart, D. E. (2007), River-mouth lagoon dynamics on mixed sand and gravel barrier coasts, *J. Coast. Res.*, *50*(ICS2007), 927–931.
Hay, W. W. (1998), Detrital sediment fluxes from continents to oceans, *Chem. Geol.*, *145*(3–4), 287–323, doi:10.1016/S0009-2541(97)00149-6.
Heathfield, D. K., and I. J. Walker (2015), Evolution of a foredune and backshore river complex on a high-energy, drift-aligned beach, *Geomorphology*, doi:10.1016/j.geomorph.2015.08.006.
Hickin, E. J., and G. C. Nanson (1984), Lateral migration rates of river bends, *J. Hydraul. Eng.*, *110*(11), 1557–1567, doi:10.1061/(ASCE)0733-9429(1984)110:11(1557).
Hicks, D. M., and D. L. Inman (1987), Sand dispersion from an ephemeral river delta on the Central California coast, *Mar. Geol.*, *77*(3–4), 305–318, doi:10.1016/0025-3227(87)90119-8.
Ismail, N. M., and R. L. Wiegel (1983), Opposing wave effect on momentum jets spreading rate, *J. Waterw. Port Coast. Ocean Eng.*, *109*(4), 465–483, doi:10.1061/(ASCE)0733-950X(1983)109:4(465.
Izumi, N., N. Shuto, and H. Tanaka (1999), Instability of river mouth locations in pocket beaches, in *Coastal Sediments '99*, edited by N. C. Kraus and W. G. McDougal, pp. 628–643, American Society of Civil Engineers, Hauppauge, N. Y.
Jerolmack, D. J., and J. B. Swenson (2007), Scaling relationships and evolution of distributary networks on wave-influenced deltas, *Geophys. Res. Lett.*, *34*, L23402, doi:10.1029/2007GL031823.
Jirka, G. H. (1994), Shallow jets, in *Recent Research Advances in the Fluid Mechanics of Turbulent Jets and Plumes*, edited by P. A. Davies and M. J. Valente Neves, pp. 155–175, Kluwer Acad., Dordrecht.
Jirka, G. H. (2001), Large scale flow structures and mixing processes in shallow flows, *J. Hydraul. Res.*, *39*(6), 567–573, doi:10.1080/00221686.2001.9628285.
Kamphuis, J. W. (1991), Alongshore sediment transport rate, *J. Waterw. Port Coast. Ocean Eng.*, *117*(6), 624–640, doi:10.1061/(ASCE)0733-950X(1991)117:6(624.
Kelk, J. G. (1974), A morphological approach to process interaction on the mid Canterbury coastline, University of Canterbury.
Kirk, R. M. (1991), River-beach interaction on mixed sand and gravel coasts: A geomorphic model for water resource planning, *Appl. Geogr.*, *11*(4), 267–287, doi:10.1016/0143-6228(91)90018-5.
Komar, P. D. (1971), Mechanics of sand transport on beaches, *J. Geophys. Res.*, *76*(3), 713–721, doi:10.1029/JC076i003p00713.
Kraus, N. C., A. Militello, and G. Todoroff (2002), Barrier beaching processes and barrier spit breach, Stone Lagoon, California, *Shore and Beach*, *70*(4), 21–28.
Leonardi, N., A. Canestrelli, T. Sun, and S. Fagherazzi (2013), Effect of tides on mouth bar morphology and hydrodynamics, *J. Geophys. Res. Oceans*, *118*, 4169–4183, doi:10.1002/jgrc.20302.
Leonardi, N., A. S. Kolker, and S. Fagherazzi (2015), Interplay between river discharge and tides in a delta distributary, *Adv. Water Resour.*, *80*, 69–78, doi:10.1016/j.advwatres.2015.03.005.
Leopold, L. B., and M. G. Wolman (1960), River meanders, *Geol. Soc. Am. Bull.*, *71*(6), 769, doi:10.1130/0016-7606(1960)71[769:RM]2.0.CO;2.
Lesser, G. R., J. A. Roelvink, J. A. T. M. Kester, and G. S. Stelling (2004), Development and validation of a three-dimensional morphological model, *Coast. Eng.*, *51*, 883–915, doi:10.1016/j.coastaleng.2004.07.014.
List, J. H., and A. D. Ashton (2007), A circulation modeling approach for evaluating the conditions for shoreline instabilities, in *Coastal Sediments '07*, edited by N. C. Kraus and J. D. Rosati, pp. 1–14, American Society of Civil Engineers, New Orleans, La.
Mariotti, G., F. Falcini, N. Geleynse, M. Guala, T. Sun, and S. Fagherazzi (2013), Sediment eddy diffusivity in meandering turbulent jets: Implications for levee formation at river mouths, *J. Geophys. Res. Earth Surf.*, *118*, 1908–1920, doi:10.1002/jgrf.20134.
Nardin, W., and S. Fagherazzi (2012), The effect of wind waves on the development of river mouth bars, *Geophys. Res. Lett.*, *39*, L12607, doi:10.1029/2012GL051788.
Nardin, W., G. Mariotti, D. A. Edmonds, R. Guercio, and S. Fagherazzi (2013), Growth of river mouth bars in sheltered bays in the presence of frontal waves, *J. Geophys. Res. Earth Surf.*, *118*, 872–886, doi:10.1002/jgrf.20057.
Nienhuis, J. H. (2016), *Plan-View Evolution of Wave-Dominated Deltas*, Massachusetts Institute of Technology and Woods Hole Oceanographic Institution, Woods Hole, Mass.

Nienhuis, J. H., A. D. Ashton, P. C. Roos, S. J. M. H. Hulscher, and L. Giosan (2013), Wave reworking of abandoned deltas, *Geophys. Res. Lett.*, *40*, 5899–5903, doi:10.1002/2013GL058231.

Nienhuis, J. H., A. D. Ashton, W. Nardin, S. Fagherazzi, and L. Giosan (2015a), Breaking-wave driven sediment bypassing of river mouths: mechanisms and effects on delta evolution, in *The Proceedings of the Coastal Sediments 2015*, edited by P. Wang, J. Rosati, and J. Cheng, World Scientific Pub Co Inc, San Diego.

Nienhuis, J. H., A. D. Ashton, and L. Giosan (2015b), What makes a delta wave-dominated?, *Geology*, *43*(6), 511–514, doi:10.1130/G36518.1.

Olabarrieta, M., W. R. Geyer, and N. Kumar (2014), The role of morphology and wave-current interaction at tidal inlets: An idealized modeling analysis, *J. Geophys. Res. Oceans*, *119*, 8818–8837, doi:10.1002/2014JC010191.

Parker, G. (1978), Self-formed straight rivers with equilibrium banks and mobile bed. Part 1. The sand-silt river, *J. Fluid Mech.*, *89*(01), 109–125, doi:10.1017/S0022112078002505.

Rodriguez, A. B., M. D. Hamilton, and J. B. Anderson (2000), Facies and evolution of the modern Brazos Delta, Texas: Wave versus flood influence, *J. Sediment. Res.*, *70*(2), 283–295, doi:10.1306/2dc40911-0e47-11d7-8643000102c1865d.

Rowland, J. C., M. T. Stacey, and W. E. Dietrich (2009), Turbulent characteristics of a shallow wall-bounded plane jet: Experimental implications for river mouth hydrodynamics, *J. Fluid Mech.*, *627*, 423, doi:10.1017/S0022112009006107.

Rowland, J. C., W. E. Dietrich, and M. T. Stacey (2010), Morphodynamics of subaqueous levee formation: Insights into river mouth morphologies arising from experiments, *J. Geophys. Res.*, *115*, F04007, doi:10.1029/2010JF001684.

Sedrati, M., P. Ciavola, and C. Armaroli (2011), Morphodynamic evolution of a microtidal barrier, the role of overwash: Bevano, Northern Adriatic Sea, *J. Coast. Res.*, *SI 64*(ICS2011), 696–700.

Stanley, D. J., and A. G. Warne (1998), Nile Delta in its destruction phase, *J. Coast. Res.*, *14*(3), 795–825.

Syvitski, J. P. M. M., and Y. Saito (2007), Morphodynamics of deltas under the influence of humans, *Global Planet. Change*, *57*(3–4), 261–282, doi:10.1016/j.gloplacha.2006.12.001.

Tanaka, H. (2003), Mathematical modelling of morphological change at a river mouth, in *International Conference on Estuaries and Coasts*, pp. 87–98, Hangzhou, China.

Tanaka, H., F. Takahashi, and A. Takahashi (1996), Complete closure of the Nanakita River mouth in 1994, in *Coastal Engineering Proceedings, Vol. 25*, edited by B. L. Edge, pp. 4545–4556, ASCE, Orlando.

van Rijn, L. C. (1993), *Principles of Sediment Transport in Rivers, Estuaries and Coastal Seas*, 1st ed., Aqua Publications, Amsterdam.

Warrick, J. A., and P. L. Barnard (2012), The offshore export of sand during exceptional discharge from California rivers, *Geology*, *40*(9), 787–790, doi:10.1130/G33115.1.

Wolman, M. G., and J. P. Miller (1960), Magnitude and frequency of forces in geomorphic processes, *J. Geol.*, *68*(1), 54–74.

Wright, L. D. (1977), Sediment transport and deposition at river mouths—A synthesis, *Geol. Soc. Am. Bull.*, *88*(6), 857–868, doi:10.1130/0016-7606(1977)88<857.

Zenkovich, V. P. (1967), *Processes of Coastal Development*, 1st ed., edited by J. A. Steers, Oliver & Boyd, Edinburgh.